

# Non-Born–Oppenheimer trajectories with self-consistent decay of mixing

Chaoyuan Zhu, Ahren W. Jasper, and Donald G. Truhlar

*Department of Chemistry and Supercomputing Institute, University of Minnesota, Minneapolis, Minnesota 55455-0431*

(Received 24 November 2003; accepted 22 December 2003)

A semiclassical trajectory method, called the self-consistent decay of mixing (SCDM) method, is presented for the treatment of electronically nonadiabatic dynamics. The SCDM method is a modification of the semiclassical Ehrenfest (SE) method (also called the semiclassical time-dependent self-consistent-field method) that solves the problem of unphysical mixed final states by including decay-of-mixing terms in the equations for the evolution of the electronic state populations. These terms generate a force, called the decoherent force (or dephasing force), that drives the electronic component of each trajectory toward a pure state. Results for several mixed quantum–classical methods, in particular the SCDM, SE, and natural-decay-of-mixing methods and several trajectory surface hopping methods, are compared to the results of accurate quantum mechanical calculations for 12 cases involving five different fully dimensional triatomic model systems. The SCDM method is found to be the most accurate of the methods tested. The method should be useful for the simulation of photochemical reactions. © 2004 American Institute of Physics. [DOI: 10.1063/1.1648306]

## I. INTRODUCTION

There is no totally consistent way to combine quantum mechanics for a subset of the degrees of freedom of a system with classical mechanics for the complementary subset. This poses a challenge for semiclassical theories of non-Born–Oppenheimer dynamics—i.e., electronically nonadiabatic processes, where electronic motions are treated quantum mechanically, and nuclear motions are treated by classical or quasiclassical methods.<sup>1–3</sup> Consequently, a large number of approximate methods for treating coupled electronic and nuclear motions have been put forward; since several monographs and reviews<sup>1–14</sup> are available, we will not include a summary of all available methods here.

A formally appealing approach to treating such problems is the semiclassical Ehrenfest (SE) method,<sup>8,10–19</sup> in which the potential governing the classical nuclear motion is the expectation value of the Hamiltonian for the quantal degrees of freedom; this is also called the time-dependent self-consistent-field method or the time-dependent Hartree method, and it is the most pristine member of a general class of methods called mean-field methods or self-consistent-potential methods. When the average potential for the quantal degrees of freedom is computed from an ensemble of trajectories, the method becomes inaccurate as the trajectories separate in space and the average becomes meaningless.<sup>20</sup> When the classical mechanical part of the system is described by independent trajectories, the method becomes more accurate,<sup>18</sup> but the inability of a mixed classical–quantum method to properly handle coherence and decoherence remains a serious defect. In particular, the lack of decoherence means that individual trajectories end in a mixed state and the distribution of energy in the classical degrees of freedom is not consistent with the quantized nature of the quantal degrees of freedom. When the quantal

degrees of freedom are the electronic degrees of freedom of a molecule, the energy spacings are often large compared to the nuclear kinetic energies, and this inconsistency makes the energy distributions qualitatively unreasonable. In a recent paper,<sup>21</sup> we introduced a decay-of-mixing method called natural decay of mixing (NDM), which includes decoherence effects in the SE method by adding an artificial force term, called the decoherent force. The decay-of-mixing method employs a switching algorithm to determine the pure state toward which the decoherent force drives the system. We showed<sup>21</sup> that the decay-of-mixing method gives more accurate results than the SE method and is comparable in accuracy to or more accurate than Tully's fewest switches (TFS) version<sup>10,22</sup> of the more popular trajectory surface hopping (TSH) approach. Unlike TSH methods, the decay-of-mixing trajectories never undergo discontinuous changes in momenta.

The attractive features of the decay-of-mixing method encouraged us to study it further, and in a later paper<sup>23</sup> we extended it to permit calculations in the adiabatic representation; this extension takes advantage of the adiabatic-to-diabatic transformation, but the system decays to adiabatic states, which is sometimes physically more reasonable than decaying to diabatic states. In further work on a system with a conical intersection,<sup>24</sup> we found that the decay-of-mixing method is much less sensitive to the choice of representation than are TSH calculations, which is encouraging because an accurate quantum mechanical calculation of the dynamics would be independent of the representation. (Semiclassical Ehrenfest trajectories are completely independent of representation,<sup>15</sup> which is one consideration in favor of this approach, but as mentioned above, they predict unrealistic product energy distributions because they do not end in a pure state, a problem that is corrected in the decay-of-mixing method by adding decoherence.) In the present article we

introduce three improvements to the decay-of-mixing method:

- (i) We make the switching algorithm locally self-consistent in the Ehrenfest (time-dependent Hartree) sense.
- (ii) We present a more satisfactory choice for the *direction* of the decoherent force.
- (iii) We introduce a new geometry dependence for the decoherence time that satisfies physically correct limits for large and small kinetic energy.

Because these improvements make the method more self-consistent and to emphasize that the method is an improved version of the time-dependent self-consistent field method,<sup>8,10–19</sup> the method is called the self-consistent decay of mixing (SCDM) method.

We note that decoherence, dephasing, and decay of mixing all refer to the tendency of a coupled state system to evolve into a statistical mixture<sup>25</sup> of pure states. In the present application the states in question are those labeling the reduced electronic density matrix in which nuclear motion has been integrated out. We simulate this decoherence by representing the quantum-mechanical wave packet as a set of independent semiclassical trajectories. The ensemble of semiclassical trajectories evolves to a set of pure states, which, taken together, represent the statistical mixture of final states of the quantum-mechanical system. Although there is a close connection between physical decoherence or dephasing and the algorithmic decay of mixing required for the set of final states of the trajectories to simulate the final state of the quantum-mechanical system, the reader should keep in mind that the algorithmic demixing considered here is not necessarily identical to physical decoherence. Therefore the only check of whether the approximations we employ for treating the decoherence time are reasonable is to compare the results of the semiclassical calculations employing our algorithm to accurate quantum dynamics. Furthermore, although the decoherence language is useful to emphasize the *connections* between the decay of mixing and decoherence, others might want to emphasize the distinctions by replacing “decoherence,” “decoherent force,” and “decoherent state” by “decay of mixing,” “demixing force,” and “pure state,” respectively.

Dephasing refers to the physical effect of damping out the coherence. Decay of mixing refers to the gradual switching from an SE trajectory to an ensemble of single-surface trajectories. The electronic coherences are the off-diagonal elements  $\rho_{ij}$  of the density matrix; when these are significant, the resulting motion is best described by the fully coherent SE method. As the system dephases and these off-diagonal elements tend to 0, the nuclear motion in the two states is no longer coherent, and the SE trajectory may be replaced with an ensemble of single-surface trajectories. It is therefore reasonable that these two processes (one physical and one algorithmic) occur at about the same rate.

We also direct the readers' attention to recent papers by Rossky and co-workers,<sup>26–28</sup> which were the first papers to elucidate the picture of the classical degrees of freedom serving as a “bath” that decoheres the electronic reduced density

matrix. In recent papers, Rossky and co-workers have also formulated a self-consistent independent-trajectory method that includes decoherence, with a special emphasis on solvent effects.<sup>28,29</sup> Ultimately one might be able to model decoherence better by a trajectory method where the quantum evolution depends on a swarm of trajectories,<sup>30–32</sup> but at present such methods are less practical for complex systems, and so we will not consider them further in the present paper.

In the present paper, in addition to introducing physical improvements in the method, we present a new way of carrying out calculations in the adiabatic representation that does not require knowing the adiabatic-to-diabatic transformation. We also reformulate the decay-of-mixing algorithm in terms of density matrices. These reformulations are convenient in some cases, especially for the multistate case, where a unitary transformation of the electronic Hamiltonian does not in general correspond to a canonical transformation of the classical-like particle representation.<sup>33</sup>

Although we discuss the NDM and SCDM methods as hybrid quantum–classical methods, in practice we use quantized initial conditions for the classical degrees of freedom. This is usually called a quasiclassical treatment,<sup>2,34,35</sup> and in this sense the hybrid methods can be called quantum and quasiclassical.

Section II presents the new SCDM theory. Section III presents test cases for three-dimensional atom–diatom collisions. Section IV gives numerical details of the semiclassical trajectory calculations. The remaining sections contain systematic tests of the methods, discussion, and concluding remarks.

## II. THEORY

We will present the theory for both adiabatic and diabatic representations. The matrix elements of the electronic Hamiltonian  $H_{\text{el}}$ , including nuclear repulsion, are the potential energy surfaces and are called  $U_{kk'}$ , where  $k$  and  $k'$  label electronic states:

$$U_{kk'} = \langle k | H_{\text{el}} | k' \rangle. \quad (1)$$

The number of states is called  $m$ , so  $k = 1, 2, \dots, m$ . We solve the equations in an isoinertial, mass-scaled nuclear coordinate system  $\mathbf{R}$  in which all nuclear masses are scaled to the same reduced mass  $\mu$ . The nonadiabatic coupling  $\mathbf{d}$  is an  $m \times m$  anti-Hermitian matrix in state space  $k$ , and each element is a vector in  $\mathbf{R}$ :

$$\mathbf{d}_{kk'} = \langle k | \nabla_{\mathbf{R}} | k' \rangle. \quad (2)$$

The momentum conjugate to  $\mathbf{R}$  is called  $\mathbf{P}$ . In the adiabatic approximation,  $\mathbf{U}$  is a diagonal matrix called  $\mathbf{V}$ , and in a diabatic representation,  $\mathbf{d}_{kk'}$  is neglected by definition.

In the present paper the diabatic representations are defined as having  $\mathbf{d}_{kk'}$  equal to zero (which is possible for realistic representations of strong-coupling regions, but which could not be true for an exact treatment of the electronic motion<sup>36–38</sup>). The nonadiabatic coupling vector in the adiabatic representation is an important quantity even for calculations carried out in the diabatic representation. When the nonadiabatic coupling is neglected or defined to be zero in the diabatic representation, then the nonadiabatic coupling

in the adiabatic representation is derived entirely from the diabatic-to-adiabatic transformation. In the rest of this paper,  $\mathbf{d}_{kk'}$  always refers to the part of the nonadiabatic coupling in the adiabatic representation that comes from the diabatic-to-adiabatic transformation. Since  $\mathbf{d}_{kk'}$  defined this way is large in strong-coupling regions, we use it as a criterion of strong coupling in both representations.

We remove the irrelevant straight-line motion of the center of total mass, and the momentum may be written as<sup>39</sup>

$$\mathbf{P} = \mathbf{P}_{\text{vib}} + \mathbf{P}_{\text{rot}}, \quad (3)$$

where  $\mathbf{P}_{\text{vib}}$  is the local vibrational momentum, and  $\mathbf{P}_{\text{rot}}$  is the linear momentum associated with the overall rotational motion. Note that for a collision process, the initial *relative* translational motion of the reagents is considered a vibrational motion in this decomposition. The instantaneous vibrational kinetic energy is given by

$$T_{\text{vib}} = \frac{P_{\text{vib}}^2}{2\mu}, \quad (4)$$

where  $P_{\text{vib}}$  is the magnitude of  $\mathbf{P}_{\text{vib}}$ . The decomposition (3) is presented in a previous article.<sup>39</sup>

As reviewed in the Introduction, the tendency of state populations to evolve to a statistical mixture of pure states (this tendency is called decay of mixing) is assumed to be governed by the time for decay of the various electronic coherences. Both processes are assumed to be first order and to be governed by the same rate matrix. In particular, the rates are determined by a matrix with elements  $\tau_{kk'}$ , which are called the decay-of-mixing relaxation times; their reciprocals are first-order rate constants. The decay-of-mixing algorithm is a modification of the semiclassical Ehrenfest method,<sup>15</sup> and the SE method is reviewed in Sec. II A. Several properties of the decay-of-mixing algorithm are derived in Sec. II B by requiring conservation of energy, angular momentum, probability, and electronic phase angle. These considerations leave undetermined the following three choices: (i) the relaxation time matrix, (ii) the direction  $\hat{\mathbf{s}}$  (in nuclear momentum space), called the decoherent direction, into which electronic energy is deposited or from which it is removed as the mixing decays, and (iii) the method for determining (as a function of time  $t$ ) the state, called the decoherent state or  $K$ , towards which the system is decohering. (Note that a caret denotes a unit vector.) Sections II A and II B present the theory in the diabatic representation, and a way of treating the adiabatic representation is given in Sec. II C. The decay of mixing equations is presented in the density matrix formalism in Sec. II D. In Sec. II E, the previously implemented<sup>21</sup> version of the decay of mixing algorithm called the natural decay of mixing method is discussed. In Sec. II F, we present the details of the improved decay-of-mixing algorithm, called self-consistent decay of mixing.

## II. A. Semiclassical Ehrenfest method

The Hamiltonian for the semiclassical Ehrenfest method  $H^{\text{SE}}$  is defined in the diabatic electronic representation as the sum of the classical nuclear kinetic energy  $T_{\text{N}}$  and the expectation value of the electronic Hamiltonian  $H_{\text{el}}$ :

$$H^{\text{SE}} = T_{\text{N}} + \langle \Psi | H_{\text{el}} | \Psi \rangle, \quad (5)$$

where the electronic Hamiltonian contains the electronic kinetic energy and the Coulomb interactions. If the electronic wave function  $\Psi$  is expanded in the diabatic basis,

$$\Psi = \sum_k c_k |k\rangle, \quad (6)$$

and the complex expansion coefficients are written in the classical-like particle representation<sup>15,33</sup> as

$$c_k = \frac{1}{\sqrt{2}} (x_k + ip_k), \quad (7)$$

Eq. (5) can be written

$$H^{\text{SE}} \equiv T_{\text{N}} + V^{\text{SE}}, \quad (8)$$

where

$$V^{\text{SE}} = \sum_k n_k U_{kk} + \sum_k \sum_{k' < k} (x_k x_{k'} + p_k p_{k'}) U_{kk'} \quad (9)$$

and where the electronic state population  $|c_k|^2$  of state  $k$  is

$$n_k = \frac{1}{2} (x_k x_k + p_k p_k). \quad (10)$$

The nuclear position and momentum of an SE trajectory evolve according to classical equations of motion

$$\dot{\mathbf{R}} = \mathbf{P}/\mu, \quad (11)$$

$$\dot{\mathbf{P}} = \dot{\mathbf{P}}^{\text{SE}} = -\nabla_{\text{N}} V^{\text{SE}}, \quad (12)$$

where the overdot indicates differentiation with respect to time, and  $\nabla_{\text{N}}$  is the nuclear gradient. The electronic variables evolve according to the time-dependent Schrödinger equation, which becomes<sup>15</sup>

$$\dot{x}_k = \dot{x}_k^{\text{SE}} = p_k U_{kk} + \sum_{k' \neq k} p_{k'} U_{kk'}, \quad (13)$$

$$\dot{p}_k = \dot{p}_k^{\text{SE}} = -x_k U_{kk} - \sum_{k' \neq k} x_{k'} U_{kk'}. \quad (14)$$

We note that Miller and Meyer proposed<sup>15,33</sup> a Langer-type modification to the SE method, in which the substitution  $n_k \rightarrow n_k + \frac{1}{2}$  is made in the electronic variables. The resulting Hamiltonian is further modified such that eigenvalues of the Hamiltonian matrix equal those obtained from the SE method. Each trajectory, then, depends on the initial value of the electronic phase angle in addition to the initial values of the nuclear position and momentum. Results are obtained by averaging over all three of these quantities. We have previously tested this method, which we call the classical electron (CE) method, and in all cases we found it to give results that are either similar to or worse than those obtained by the SE method.<sup>42</sup> We do not consider the CE method any further in the present paper.

## II.B. Semiclassical Ehrenfest method with decay of mixing

The decay of mixing algorithm modifies the SE equations of motion (12)–(14) such that the system decays continuously to a pure state. In particular, the equation of motion for the nuclear position is unchanged [Eq. (11)], but those for the momentum and the electronic variables  $x_k$  and  $p_k$  become

$$\dot{\mathbf{P}} = \dot{\mathbf{P}}^{\text{SE}} + \dot{\mathbf{P}}^{\text{D}}, \quad (15)$$

$$\dot{x}_k = \dot{x}_k^{\text{SE}} + \dot{x}_k^{\text{D}}, \quad (16)$$

$$\dot{p}_k = \dot{p}_k^{\text{SE}} + \dot{p}_k^{\text{D}}. \quad (17)$$

Several properties of the decoherence terms  $\dot{\mathbf{P}}^{\text{D}}$ ,  $\dot{x}_k^{\text{D}}$ , and  $\dot{p}_k^{\text{D}}$  are discussed in the following subsections. First, however, we note that the SE labels on the first terms of Eqs. (15)–(17) refer to the local time derivative only. When one includes the decoherence terms, the trajectory immediately deviates from the SE one, and so  $\dot{x}_k^{\text{SE}}$  and  $\dot{p}_k^{\text{SE}}$  here are different from their values along the SE trajectory.

### II.B.1. Conservation of total angular momentum and energy

The time derivative of the total angular momentum

$$\mathbf{J} = \mathbf{R} \times \mathbf{P} \quad (18)$$

can be written

$$\dot{\mathbf{J}} = \dot{\mathbf{R}} \times \mathbf{P} + \mathbf{R} \times \dot{\mathbf{P}} = \frac{\mathbf{P}}{\mu} \times \mathbf{P} + \mathbf{R} \times \dot{\mathbf{P}}^{\text{SE}} + \mathbf{R} \times \dot{\mathbf{P}}^{\text{D}}, \quad (19)$$

where we have used Eqs. (11) and (15). (Note that  $\dot{\mathbf{R}}^{\text{D}}$  is zero.) The first two terms correspond to SE motion, and the SE method has previously been shown to conserve total angular momentum.<sup>15</sup> By requiring the decay-of-mixing method to conserve total angular momentum, we therefore obtain

$$\mathbf{R} \times \dot{\mathbf{P}}^{\text{D}} = 0 \quad (20)$$

or, equivalently,

$$\dot{\mathbf{P}}^{\text{D}} = F \hat{\mathbf{s}}, \quad (21)$$

where  $F$  is an undetermined scalar function and  $\hat{\mathbf{s}}$  is a unit vector that lies within the nonrotating subspace of momentum space: i.e.,  $\hat{\mathbf{s}}$  must be chosen such that

$$\mathbf{R} \times \hat{\mathbf{s}} = 0. \quad (22)$$

The time derivative of the Hamiltonian is

$$\begin{aligned} \dot{H} &= \frac{d}{dt}(T_{\text{N}} + V) \\ &= \frac{\mathbf{P} \cdot \dot{\mathbf{P}}}{\mu} + \dot{V}^{\text{DM}} \\ &= \frac{\mathbf{P} \cdot \dot{\mathbf{P}}^{\text{SE}}}{\mu} + \dot{V}^{\text{SE}} + \frac{\mathbf{P} \cdot \dot{\mathbf{P}}^{\text{D}}}{\mu} + \dot{V}^{\text{D}}, \end{aligned} \quad (23)$$

where  $\dot{V}^{\text{DM}}$  is the time derivative of the classical potential energy,

$$V^{\text{DM}} = \sum_k n_k U_{kk} + \sum_k \sum_{k' < k} (x_k x_{k'} + p_k p_{k'}) U_{kk'}, \quad (24)$$

and has been written

$$\dot{V}^{\text{DM}} = \dot{V}^{\text{SE}} + \dot{V}^{\text{D}} \quad (25)$$

using Eqs. (16) and (17). Note that Eq. (24) differs from Eq. (9) because the  $x_k$  and  $p_k$  variables in Eq. (9) evolve according to Eqs. (13) and (14), whereas the  $x_k$  and  $p_k$  variables in Eq. (24) evolve according to Eqs. (16) and (17). Therefore,<sup>21</sup>

$$\begin{aligned} \dot{V}^{\text{D}} &= \frac{1}{2} \sum_k (x_k \dot{x}_k^{\text{D}} + p_k \dot{p}_k^{\text{D}}) U_{kk} + \sum_k \sum_{k' < k} (x_k \dot{x}_{k'}^{\text{D}} + x_{k'} \dot{x}_k^{\text{D}} \\ &\quad + p_k \dot{p}_{k'}^{\text{D}} + p_{k'} \dot{p}_k^{\text{D}}) U_{kk'}. \end{aligned} \quad (26)$$

The first two terms on the right-hand side of Eq. (23) correspond to SE motion and conserve total energy.<sup>15</sup> For the decay-of-mixing algorithm to conserve total energy the sum of the two remaining terms must equal zero, and using Eq. (21), we therefore obtain

$$F = \frac{-\dot{V}^{\text{D}}}{\mathbf{P} \cdot \hat{\mathbf{s}} / \mu}, \quad (27)$$

and the change in nuclear momentum due to decoherence is

$$\dot{\mathbf{P}}^{\text{D}} = -\frac{\mu \dot{V}^{\text{D}}}{\mathbf{P} \cdot \hat{\mathbf{s}}} \hat{\mathbf{s}}. \quad (28)$$

Thus the right-hand side of Eq. (28) is the decoherent force. Note that  $\dot{\mathbf{P}}^{\text{D}}$  becomes singular (undefined) as  $\mathbf{P} \cdot \hat{\mathbf{s}} \rightarrow 0$  unless this singularity is cancelled by a zero of  $\dot{V}^{\text{D}}$ ; this constrains our choice of the direction  $\hat{\mathbf{s}}$ . We will choose  $\hat{\mathbf{s}}$  in Sec. II C such that  $\mathbf{P} \cdot \hat{\mathbf{s}}$  only equals zero when  $\mathbf{P}_{\text{vib}}$  is the null vector. In the semiclassical Ehrenfest method, as in an ordinary trajectory, the various components of  $\mathbf{P}_{\text{vib}}$  will not equal zero simultaneously, and hence the variables  $P_{\text{vib}}$  and  $T_{\text{vib}}$  will not pass through zero. However, in the decay-of-mixing algorithm, the decoherent force can drive  $P_{\text{vib}}$  toward zero in some regions of space. To prevent the right-hand side of Eq. (28) from becoming singular,  $\dot{V}^{\text{D}}$  must go to zero faster than the denominator. Thus  $\dot{V}^{\text{D}}$  must be an explicit function of  $P_{\text{vib}}$ , which, for small  $P_{\text{vib}}$ , varies as  $P_{\text{vib}}^n$  with  $n > 1$ . In practice, we have found that  $n = 2$  is sufficient to prevent this problem (we did not examine fractional values like 1.5).

We note that Eq. (28) can be generalized to

$$\dot{\mathbf{P}}^{\text{D}} = \sum_k \dot{\mathbf{P}}_k^{\text{D}} = -\sum_k \frac{\mu \dot{V}_k^{\text{D}}}{\mathbf{P} \cdot \hat{\mathbf{s}}_k} \hat{\mathbf{s}}_k, \quad (29)$$

where  $\dot{V}_k^{\text{D}}$  is the contribution to  $\dot{V}^{\text{D}}$  from state  $k$ , and we have allowed the direction of the decoherent force  $\hat{\mathbf{s}}_k$  to depend on the electronic state  $k$ . We will consider Eq. (29) in more detail in Sec. II F 1.

### II.B.2. First-order decay and conservation of probability and phase angle

We assume that the decay of the electronic state populations is first order and that there is some electronic state  $K$  toward which the system is decohering. A set of decoherence



times  $\tau_{kK}$  is defined such that the electronic state population  $n_k$  for  $k \neq K$  decays to zero at a rate of  $1/\tau_{kK}$ —i.e.,

$$\dot{n}_k^D = -\frac{n_k}{\tau_{kK}} \quad \text{for } k \neq K. \quad (30)$$

To ensure conservation of probability, we set

$$\sum_k \dot{n}_k = \sum_k \dot{n}_k^{\text{SE}} + \sum_k \dot{n}_k^D = 0. \quad (31)$$

The SE terms conserve probability,<sup>15</sup> so

$$\sum_k \dot{n}_k^D = \sum_{k \neq K} \dot{n}_k^D + \dot{n}_K^D = 0, \quad (32)$$

and therefore

$$\dot{n}_K^D = -\sum_{k \neq K} \dot{n}_k^D = \sum_{k \neq K} \frac{n_k}{\tau_{kK}}. \quad (33)$$

The electronic phase angle  $q_k$  is defined by

$$\tan q_k = \frac{p_k}{x_k}, \quad (34)$$

and the contribution to its time derivative from the decay terms is

$$\left. \frac{d}{dt} (\tan q_k) \right|_D = \frac{x_k \dot{p}_k^D - \dot{x}_k p_k}{x_k^2}. \quad (35)$$

Requiring conservation of phase angle gives

$$\frac{\dot{p}_k^D}{p_k} = \frac{\dot{x}_k}{x_k}. \quad (36)$$

From Eqs. (10), (30), (33), and (36) we can derive expressions for  $\dot{x}_k^D$  and  $\dot{p}_k^D$ . For  $k \neq K$ ,

$$\dot{p}_k^D = -\frac{p_k}{2\tau_{kK}}, \quad (37)$$

$$\dot{x}_k^D = -\frac{x_k}{2\tau_{kK}}, \quad (38)$$

and for state  $K$ ,

$$\dot{p}_K^D = \frac{p_K}{2n_K} \sum_{k \neq K} \frac{n_k}{\tau_{kK}}, \quad (39)$$

$$\dot{x}_K^D = \frac{x_K}{2n_K} \sum_{k \neq K} \frac{n_k}{\tau_{kK}}. \quad (40)$$

For later reference we note that, for any  $k$ , the contribution of decoherence to the electronic state population is

$$\dot{n}_k^D = \dot{n}_k - \dot{n}_k^{\text{SE}} = x_k \dot{x}_k^D + p_k \dot{p}_k^D. \quad (41)$$

After requiring a first-order decay of the electronic state populations and enforcing conservation of energy, angular momentum, probability, and phase angle, the remaining undetermined parameters are the direction  $\hat{s}$  [or the set of  $\hat{s}_k$  if the more general Eq. (29) is used] of the energy exchange due to decoherence and the set of decoherence times  $\tau_{kK}$ . We also need a method for determining the decoherent state  $K$ —that is, for switching from one decoherent state to an-

other as the trajectory proceeds in such a way that on average the ensemble of trajectories produces a statistical mixture of pure states that agrees as well as possible with an accurate quantum-mechanical calculation.

Putting Eqs. (37)–(40) into Eq. (26) shows that every term in  $\dot{V}^D$  is proportional to one or another  $\tau_{kk'}^{-1}$ . Thus the requirement in the previous subsection that, for small  $P_{\text{vib}}$ ,  $\dot{V}^D$  varies as  $P_{\text{vib}}^n$  with  $n \geq 2$  leads to a requirement that, for small  $P_{\text{vib}}$ , each  $\tau_{kk'}$  varies as  $P_{\text{vib}}^{-n}$  with  $n \geq 2$ .

## II.C. Decay of mixing in the adiabatic representation

So far, we have limited our discussion to the diabatic electronic representation. In this section, we consider applying the decay-of-mixing algorithm in a general representation that includes the diabatic and adiabatic representations as special cases, and then we specialize to the adiabatic case. For a general basis, the solution to the time-dependent Schrödinger equation is<sup>22</sup>

$$i\hbar \dot{c}_k = \sum_{k'} c_{k'} (U_{kk'} - i\hbar \dot{\mathbf{R}} \cdot \mathbf{d}_{kk'}). \quad (42)$$

The coupled equations (42) reduce to the diabatic representation if  $\mathbf{d}_{kk'} = 0$ , and they yield the adiabatic representation if  $U_{kk'} = 0$  for  $k \neq k'$ , in which case  $U_{kk}$  is called  $V_k$ . Substituting the complex expansion coefficients, Eq. (7) into Eq. (42), we have

$$\dot{x}_k^{\text{SE}} = \sum_{k'} (\hbar^{-1} p_{k'} U_{kk'} - x_{k'} \dot{\mathbf{R}} \cdot \mathbf{d}_{kk'}), \quad (43)$$

$$\dot{p}_k^{\text{SE}} = -\sum_{k'} (\hbar^{-1} x_{k'} U_{kk'} + p_{k'} \dot{\mathbf{R}} \cdot \mathbf{d}_{kk'}). \quad (44)$$

The decoherent contributions to the rate of change of these generalized coordinates are obtained using Eqs. (37)–(40) and are added to Eqs. (43) and (44) to obtain the overall electronic motion by Eqs. (16) and (17). The nuclear coordinates and momenta satisfy Eqs. (11) and (15) with

$$\begin{aligned} \dot{\mathbf{P}}^{\text{SE}} = & -\sum_k n_k \nabla_{\mathbf{R}} U_{kk} - \sum_k \sum_{k' < k} (x_k x_{k'} + p_k p_{k'}) \nabla_{\mathbf{R}} U_{kk'} \\ & + \sum_j \sum_k \sum_{k'} (x_k x_{k'} + p_k p_{k'}) U_{kk'} \mathbf{d}_{k'j}. \end{aligned} \quad (45)$$

In the adiabatic representation, Eq. (45) reduces to an expression derived by Tully,<sup>1</sup> namely,

$$\dot{\mathbf{P}}^{\text{SE}} = -\sum_k n_k \nabla_{\mathbf{R}} V_k + \sum_k \sum_{k'} c_k^* c_{k'} (V_k - V_{k'}) \mathbf{d}_{kk'}, \quad (46)$$

in which  $n_k$  is defined in Eq. (10), but here it represents the electronic-state population in the adiabatic representation. [Note that we corrected a sign error in Tully's equation (6.26); Eq. (46) is derived in the Appendix.] The force and momentum derivative associated with the decoherence are given by Eqs. (26)–(29). Conservation of total energy and angular momentum and conservation of density and phase angle for electronic states in a general representation can be proved in the same way as in Secs. II B 1 and II B 2 for the diabatic representation, respectively.

The advantage of the adiabatic formulation presented here over the one presented in Ref. 23 is that the present treatment does not require one to know the adiabatic–diabatic transformation. The two formulations give identical trajectories and electronic probabilities for systems with two electronic states; one can use whichever formulation is more convenient. For systems with more than two electronic states, matrix elements of the nuclear kinetic energy operator couple the adiabatic electronic states in addition to the momentum coupling that already occurs in the two-state case. These terms are neglected in the present treatment, but are included (nonuniquely) in the treatment in Ref. 23. This ambiguity in the semiclassical electronic state formulation is endemic to the formulation of the problem in which quantal degrees of freedom are coupled to classical ones in a classical-like framework.<sup>33</sup> Nevertheless, Eq. (46) has the advantage that it is independent of the nonunique adiabatic-to-diabatic transformation (the transformation is nonunique because a strictly diabatic representation does not exist<sup>36–38</sup>). One (nonunique) way to resolve the latter ambiguity is to define the problem in the diabatic representation and assume that the entire nonadiabatic coupling results from the diabatic-to-adiabatic transformation<sup>5,36,40–44</sup> (retaining the longitudinal part due to the transformation but neglecting the remaining longitudinal part and all of the transverse part<sup>36</sup>), but further discussion of this aspect of the problem is beyond our scope. We simply remark that the formulation in this section is preferred because it is equally applicable whether one defines the problem in a diabatic representation where nonadiabatic coupling vanishes or in an adiabatic representation that includes both longitudinal and transverse nonadiabatic coupling. Other problems arise, however, if the nonadiabatic coupling does not vanish in asymptotic regions, and we implicitly assume that it does. We also neglect electronic angular momentum.

## II.D. Density matrix formulation

So far, we have presented the decay of mixing formalism in the particle representation of Ref. 15. It is also useful to present the equations in density matrix language. The two treatments give identical results.

The elements of the electronic density matrix are

$$\rho_{ij} = c_i c_j^*, \quad (47)$$

where  $c_i$  is defined in Eq. (7) and  $c_j^*$  is the complex conjugate of  $c_j$ . Using Eq. (7), we obtain

$$\begin{aligned} \text{Im}(\rho_{ij}) &= \frac{1}{2}(x_j p_i - x_i p_j), \\ \text{Re}(\rho_{ij}) &= \frac{1}{2}(x_i x_j + p_i p_j), \quad i \neq j, \\ n_i &\equiv \rho_{ii} = \frac{1}{2}(x_i^2 + p_i^2). \end{aligned} \quad (48)$$

The time derivative of the density matrix can be decomposed into a semiclassical Ehrenfest contribution and contribution due to the decay of mixing force:

$$\dot{\rho}_{ij} = \dot{\rho}_{ij}^{\text{SE}} + \dot{\rho}_{ij}^{\text{D}}. \quad (49)$$

Using Eqs. (16), (17), (43), and (44) one obtains, for the SE contribution,

$$i\hbar \dot{\rho}_{kj}^{\text{SE}} = \sum_l (\rho_{lj} [U_{kl} - i\hbar \dot{\mathbf{R}} \cdot \mathbf{d}_{kl}] - \rho_{kl} [U_{lj} - i\hbar \dot{\mathbf{R}} \cdot \mathbf{d}_{lj}]), \quad (50)$$

and using Eqs. (37)–(40), the decoherent contribution is given by

$$\dot{\rho}_{ii}^{\text{D}} = \begin{cases} -\frac{\rho_{ii}}{\tau_{iK}}, & i \neq K, \\ \sum_{j \neq K} \frac{\rho_{jj}}{\tau_{Kj}}, & i = K, \end{cases} \quad (51)$$

and for  $i \neq j$ ,

$$\dot{\rho}_{ij}^{\text{D}} = \begin{cases} -\frac{1}{2} \left( \frac{1}{\tau_{iK}} + \frac{1}{\tau_{jK}} \right) \rho_{ij}, & i \neq K, \quad j \neq K, \\ \frac{1}{2} \left( \frac{1}{\rho_{KK}} \sum_{k \neq K} \frac{\rho_{kk}}{\tau_{Kk}} - \frac{1}{\tau_{jK}} \right) \rho_{ij}, & i = K, \quad j \neq K, \\ \frac{1}{2} \left( \frac{1}{\rho_{KK}} \sum_{k \neq K} \frac{\rho_{kk}}{\tau_{Kk}} - \frac{1}{\tau_{iK}} \right) \rho_{ij}, & i \neq K, \quad j = K. \end{cases} \quad (52)$$

The time derivative of the nuclear momentum can be written in density matrix notation as in Eq. (15) where

$$\begin{aligned} \dot{\mathbf{P}}^{\text{SE}}(t) &= - \sum_k \rho_{kk} \nabla_{\mathbf{R}} U_{kk} - \sum_k \sum_{k' < k} (2 \text{Re } \rho_{kk'}) \nabla_{\mathbf{R}} U_{kk'} \\ &\quad + \sum_j \sum_k \sum_{k'} (2 \text{Re } \rho_{kj}) U_{kk'} \mathbf{d}_{k'j}, \end{aligned} \quad (53)$$

and  $\dot{\mathbf{P}}^{\text{D}}$  is computed using Eq. (29) and

$$\dot{V}^{\text{D}} = \sum_k \dot{\rho}_{kk}^{\text{D}} U_{kk} + \sum_k \sum_{k' < k} (2 \text{Re } \dot{\rho}_{kk'}^{\text{D}}) U_{kk'}. \quad (54)$$

## II.E. NDM

For the previously published NDM method,<sup>21</sup> the decoherent direction is independent of electronic state; i.e., Eq. (28) is used with

$$\hat{\mathbf{s}} = \frac{\mathbf{P}_{\text{vib}}}{\|\mathbf{P}_{\text{vib}}\|}, \quad (55)$$

and the relaxation times are

$$\tau_{kk'} = \tau_{kk'}^{\text{gap}} \frac{T_0}{T_{\text{vib}}}, \quad (56)$$

where

$$\tau_{kk'}^{\text{gap}} \equiv \frac{\hbar}{\Delta U_{kk'}}, \quad (57)$$

$$\Delta U_{k'k} \equiv |U_{k'k} - U_{kk}| \quad (58)$$

and  $T_0$  is a constant which we set equal to the total energy  $E$  relative to the potential energy of the reactant(s) at equilibrium.

The system starts in a pure state, and initially the decoherent state is the same as that state. The decoherent state  $K$  is dynamically determined at small time intervals  $dt$  along the classical trajectory using the fewest-switches method<sup>22</sup> and the electronic state probabilities  $n_k$ , which are  $\rho_{kk}$  in the density matrix formulation. For example, for a two-state system, the probability that a trajectory switches its decoherent state from state  $K$  to state  $K'$  at time  $t$  is

$$P_{K \rightarrow K'} = \max\left(-\frac{\dot{\rho}_{KK} dt}{\rho_{KK}}, 0\right). \quad (59)$$

The NDM method was shown to work well when tested against the SE method and several trajectory surface hopping methods.<sup>21</sup> In the next section we discuss several shortcomings of the NDM method and present the improved self-consistent decay of mixing algorithm.

## II.F. SCDM

### II.F.1. Decoherent direction

The unit vectors  $\hat{\mathbf{s}}_k$  determine the direction into which energy is deposited and out of which energy is taken as the system decoheres. Equation (55) is unsatisfactory because it can couple the electronic energy to nuclear degrees of freedom arbitrarily far from the electronically nonadiabatic moiety (i.e., the “chromophore”), even when the nonadiabatic coupling is large.

We note that Eq. (51) may be used to write Eq. (54) as

$$\dot{V}^D = \sum_{k \neq K} \dot{V}_k^D, \quad (60)$$

where

$$\begin{aligned} \dot{V}_k^D = & \frac{\rho_{kk}}{\tau_{Kk}} U_{KK} + \dot{\rho}_{kk}^D U_{kk} + (\text{Re } \dot{\rho}_{Kk}^D) U_{Kk} \\ & + \sum_{k' \neq k} (\text{Re } \dot{\rho}_{kk'}^D) U_{kk'}, \end{aligned} \quad (61)$$

and so the momentum change associated with the decoherence can be written a sum of terms [as in Eq. (29)]. Each term describes the decoherence of a single state  $k$  to the decoherent state  $K$ —i.e.,

$$\dot{\mathbf{P}}^D = - \sum_{k \neq K} \frac{\mu \dot{V}_k^D}{\mathbf{P} \cdot \hat{\mathbf{s}}_k} \hat{\mathbf{s}}_k, \quad (62)$$

where  $\hat{\mathbf{s}}_k$  is the direction of the decoherence associated with state  $k$ . This decomposition is essential for incorporating the correct mode dependence of the vibronic coupling in multi-state systems. In order to derive a physically motivated form for  $\hat{\mathbf{s}}_k$ , we consider the physical origin of the state coupling. We will do this first for the adiabatic representation and then for the diabatic representation.

*a. Adiabatic representation.* The nonadiabatic coupling drives electronic state changes in the adiabatic representation and is given by

$$C_{kk'} = (\hbar/\mu) \mathbf{P}_{\text{vib}} \cdot \mathbf{d}_{kk'}^{(\text{tot})}, \quad (63)$$

where  $\mathbf{P}_{\text{vib}}$  is the momentum associated with internal vibrational motion<sup>39</sup> and  $\mathbf{d}_{kk'}^{(\text{tot})}$  is the total nonadiabatic coupling vector given by

$$\mathbf{d}_{kk'}^{(\text{tot})} = \mathbf{d}_{kk'} + \mathbf{d}_{kk'}^{(\perp)}, \quad (64)$$

in which  $\mathbf{d}_{kk'}$  continues to denote the nonadiabatic coupling due to the diabatic–adiabatic transformation and  $\mathbf{d}_{kk'}^{(\perp)}$  is the transverse component<sup>36</sup> of the coupling, which is usually neglected (and is always neglected in the diabatic representation; however, it is reasonable to take account of it in determining the direction of  $\hat{\mathbf{s}}$ ). The vector  $\mathbf{d}_{kk'}^{(\perp)}$  is difficult to calculate, but is associated with all components of nuclear momentum and has a magnitude<sup>38</sup> of  $O(1 a_0^{-1})$ , where  $a_0$  is a bohr. We therefore approximate

$$\mathbf{d}_{kk'}^{(\perp)} \cong \pm a_0^{-1} \hat{\mathbf{P}}_{\text{vib}}, \quad (65)$$

where  $\hat{\mathbf{P}}_{\text{vib}}$  is a unitless unit vector in the direction of  $\mathbf{P}_{\text{vib}}$ . Substituting Eq. (65) into Eq. (63) gives

$$C_{kk'} = (\hbar/\mu a_0) (d_{kk'} a_0 P_{kk'}^{(\text{d})} \pm P_{\text{vib}}), \quad (66)$$

where  $d_{kk'}$  is the magnitude ( $\|\mathbf{d}_{kk'}\|$ ) of  $\mathbf{d}_{kk'}$  and  $P_{kk'}^{(\text{d})}$  is the component of  $\hat{\mathbf{P}}_{\text{vib}}$  in the direction of  $\mathbf{d}_{kk'}$ .

We associate the first term in Eq. (66) with the direction  $\hat{\mathbf{d}}_{kk'}$  and the second term with the direction  $\hat{\mathbf{P}}_{\text{vib}}$ . Thus we take

$$\hat{\mathbf{s}}_k = \hat{\mathbf{S}}_{Kk}, \quad (67)$$

where  $K$  is the decoherent state and

$$\begin{aligned} \hat{\mathbf{S}}_{Kk} = & (d_{kk'} a_0 P_{kk'}^{(\text{d})} \hat{\mathbf{d}}_{kk'} \pm P_{\text{vib}} \hat{\mathbf{P}}_{\text{vib}}) / \|d_{kk'} a_0 P_{kk'}^{(\text{d})} \hat{\mathbf{d}}_{kk'} \\ & \pm P_{\text{vib}} \hat{\mathbf{P}}_{\text{vib}}\|. \end{aligned} \quad (68)$$

The sign in Eq. (65) is arbitrary, and we choose it such that the overlap of  $\mathbf{d}_{kk'}$  and  $\mathbf{P}_{\text{vib}}$  is positive and the contributions from the two terms in Eq. (66) are additive.

Furthermore, the sign of  $\mathbf{d}_{kk'}$ , although arbitrary, is fixed by a particular choice of phase conventions for  $|k\rangle$  and  $|k'\rangle$  at the beginning of the calculation, and then those phase conventions are used continuously throughout the calculation.

When we use Eq. (67) as the decoherent direction for coupling state  $k$  to the decoherent state  $K$ , then, in regions where the surface  $K$  is strongly coupled to any other surface  $k$ , energy transfer due to decoherence takes place along  $\mathbf{d}_{Kk}$ , which may be justified by analogy with surface hopping, where it has been shown<sup>39,45,46</sup> that instantaneous surface transitions due the strong nonadiabatic coupling between states  $K$  and  $k$  involve energy adjustments along  $\mathbf{d}_{Kk}$ . In regions away from the strong-coupling region (i.e., in regions where all  $\mathbf{d}_{Kk}$  are very small), all internal vibrations of the system contribute equally to decoherence.

Both  $\mathbf{d}_{kk}$  and  $\mathbf{P}_{\text{vib}}$  are within the nonrotational subspace, and therefore momentum adjustments along  $\hat{\mathbf{s}}_k$  conserve total angular momentum, as discussed in Sec. II B 1.

*b. Diabatic representation.* Since the gradient is an anti-Hermitian operator, Eq. (2) shows that  $\mathbf{d}_{kk'} = -\mathbf{d}_{k'k}$ . With this in mind it is easy to see that Eq. (67) reduces to

$$\hat{\mathbf{s}}_k = \frac{\pm(d_{12}a_0P_{12}^{(d)}\hat{\mathbf{d}}_{12} \pm P_{\text{vib}}\hat{\mathbf{p}}_{\text{vib}})}{\|d_{12}a_0P_{12}^{(d)}d_{12} \pm P_{\text{vib}}\hat{\mathbf{p}}_{\text{vib}}\|} \quad (69)$$

in the two-state case, where the first  $\pm$  depends on whether  $K$  is 1 or 2, but cancels in Eq. (29), and the next two  $\pm$  are determined by the convention after Eq. (68). When there are only two electronic states  $\mathbf{d}_{12}$  provides a meaningful direction for the decoherent force in an adiabatic representation, as discussed above, and since there is only one pair of states, also in the diabatic representation. Based on these considerations, we generalize the above treatment to  $N$  diabatic states as follows.

In the rest of this section, let  $k$  and  $k'$  represent adiabatic states and  $j$  and  $j'$  represent diabatic states. The nonadiabatic coupling vector  $\mathbf{d}_{kk'}$  is the vector coupling between two adiabatic states  $k$  and  $k'$ , each of which is, in general, some linear combination of all of the diabatic states  $j$ . The diabatic potential energy matrix (whose elements are  $U_{jj'}$ ) is an  $N \times N$  symmetric matrix. For any pair of diabatic states, we can construct the potential energy submatrix

$$\mathbf{U}_{jj'}^{(2)} = \begin{pmatrix} U_{jj} & U_{jj'} \\ U_{jj'} & U_{j'j'} \end{pmatrix}, \quad (70)$$

which controls the direct coupling between these two states. An effective coupling  $\mathbf{d}_{jj'}^{(2)}$  may be computed using  $\mathbf{U}_{jj'}^{(2)}$  and its gradient, eigenvectors, and eigenvalues according to the usual formula for a two-state system.<sup>39</sup> To obtain  $\hat{\mathbf{s}}_{jj'}$  we use Eq. (68), replacing the adiabatic nonadiabatic coupling  $\mathbf{d}_{kk'}$  with the effective coupling  $\mathbf{d}_{jj'}^{(2)}$ .

### II.F.2. Decay-of-mixing time

The dependence of the relaxation times in Eq. (56) on  $T_0$  is unsatisfactory, and in the original paper<sup>21</sup> we identified the development of a more microscopically justified approximation for  $\tau_{kk'}$  as a direction for further study. Although, as pointed out in the Introduction, the ultimate justification for  $\tau_{kk'}$  must be comparison of the results of the semiclassical calculations employing the new algorithm to accurate quantum dynamics, we believe that the argument given next provides a more self-consistent way to introduce the vibrational kinetic energy.

The time-dependent electronic wave function may be written as

$$\Psi = \sum_k c_k(t) \phi_k(\mathbf{R}(t)) e^{-iU_{kk}(\mathbf{R}(t))t/\hbar}, \quad (71)$$

and the probability density is

$$\begin{aligned} |\Psi|^2 &= \sum_k |c_k(t)|^2 |\phi_k(\mathbf{R}(t))|^2 \\ &+ \sum_k \sum_{k' \neq k} c_k^*(t) c_{k'}(t) \phi_k^*(\mathbf{R}(t)) \\ &\times \phi_{k'}(\mathbf{R}(t)) e^{-i\Delta U_{k'k}(\mathbf{R}(t))t/\hbar}. \end{aligned} \quad (72)$$

Therefore, in the reduced electronic density matrix, the nuclear coordinates are integrated out and the differing nuclear motions of the components of the wave packet asso-

ciated with electronic states  $k$  and  $k'$  cause the element of the reduced density matrix associated with the coherence  $c_k^* c_{k'}$  to decay because of reduced overlap of the spatial components and because of destructive interference of the phase factors in Eq. (72). The equation shows that the time scale associated with this phase interference is  $\tau_{kk'}^{\text{gap}}$ , defined in Eq. (57). Except when  $\Delta U_{kk'}$  is very small, this time scale is much faster than the time scale for nuclear overlap decay, and it is the fastest time scale in the system. A central assumption of the SCDM method is that this time scale provides a lower bound to the decay-of-mixing time  $\tau_{kk'}$ . The lower bound character of  $\tau_{kk'}^{\text{gap}}$  could also be justified by the time-energy uncertainty relation. In this context a first approximation for the relaxation time is

$$\tau_{kk'}^{(1)} \approx 2\tau_{kk'}^{\text{gap}}(\mathbf{R}(t)), \quad (73)$$

where the factor of 2 accounts for the fact that a trajectory should traverse a complete passage of a strong-coupling region with maximum coherence,<sup>47,48</sup> and the decay-of-mixing time must allow significant coherence over both the approach and recession from the point of maximum interaction, hence the factor of 2.

In Sec. II A, we pointed out that, for small  $P_{\text{vib}}$ , a self-consistent treatment requires that the decoherence rate constant  $\tau_{kk'}^{-1}$  should tend to zero at least as fast as  $P_{\text{vib}}^2$ . To incorporate this requirement, we derive an alternative form of the relaxation rate matrix. At any given geometry  $\mathbf{R}$ , we associate the self-consistent trajectory with two virtual trajectories, one obtained by a virtual hop up to state  $k'$  and one by a virtual hop down to state  $k$  (the virtual hops being defined in the usual sense of trajectory surface hopping). In semiclassical methods, one assumes conservation of nuclear angular momentum during hops as well as along trajectories. Since the instantaneous rotational kinetic energy  $T_{\text{rot}}$  depends only on local geometry (through the instantaneous moments of inertia) and on angular momentum, it is conserved during hops. Therefore, the decomposition of the total energy of the virtual trajectories into kinetic and potential energy components may be written

$$E = T_{\text{vib},k} + T_{\text{rot}} + U_{kk} \quad (74)$$

and the virtual vibrational kinetic energies may be used to define vibrational momenta after the virtual hop onto each surface:

$$T_{\text{vib},k} = \frac{P_{\text{vib},k}^2}{2\mu}. \quad (75)$$

Since total energy is also conserved during a hop, one can write

$$\Delta U_{kk'} = |T_{\text{vib},k} - T_{\text{vib},k'}| = \left( \frac{\bar{P}_{\text{vib}}}{\mu} \right) \Delta P_{\text{vib},kk'}, \quad (76)$$

where

$$\bar{P}_{\text{vib}} = (P_{\text{vib},k} + P_{\text{vib},k'})/2 \quad (77)$$

and

$$\Delta P_{\text{vib},kk'} = |P_{\text{vib},k} - P_{\text{vib},k'}|. \quad (78)$$



To make this self-consistent with the SCDM trajectory, we replace the unweighted average momentum in Eq. (77) by the current self-consistent field average, which is  $P_{\text{vib}}$ —i.e., the instantaneous vibrational momentum along the current SCDM trajectory. Thus we may use

$$\Delta U'_{kk'} = \left( \frac{P_{\text{vib}}}{\mu} \right) |P_{\text{vib},k} - P_{\text{vib},k'}|, \quad (79)$$

which, combined with Eqs. (57) and (73), yields an alternative approximation

$$\tau'_{kk'} = \frac{2\hbar\mu}{P_{\text{vib}}|P_{\text{vib}} - P_{\text{vib},k}|}. \quad (80)$$

*A priori*, any expression of the form

$$\tau_{kk'} = (\tau'_{kk'})^n (\tau_{kk'}^{\text{gap}})^{1-n} \quad (81)$$

is equally suitable, although it seems reasonable to limit consideration to the smallest suitable value of  $n$  that is consistent with the decay of mixing formalism. To accomplish this we note that  $\tau_{kk'}^{\text{gap}}$  is independent of  $P_{\text{vib}}$ , but  $\tau'_{kk'} \sim P_{\text{vib}}^{-1}$ , and therefore Eq. (81) yields  $\tau_{kk'} \sim P_{\text{vib}}^{-n}$ . As explained above, the decay of mixing formula requires  $n \geq 2$ , and so we choose  $n = 2$ . This yields an alternative expression

$$\tau_{kk'}^{(2)} = \frac{\hbar\mu\Delta U'_{kk'}}{T_{\text{vib}}|P_{\text{vib},k} - P_{\text{vib},k'}|}. \quad (82)$$

This is not well defined when the virtual hop to the upper surface is forbidden by the conservation of energy or linear momentum, and so we consider a third approximation given by the limit of Eq. (82) when  $P_{\text{vib},k} \gg P_{\text{vib},k'}$ . This yields

$$\tau_{kk'}^{(3)} = \frac{\hbar}{2T_{\text{vib}}}. \quad (83)$$

Both  $\tau_{kk'}^{(1)}$  and  $\tau_{kk'}^{(3)}$  are well defined in all cases, but neither of them alone satisfies all the physical constraints we require for  $\tau_{kk'}$ . However, an arithmetic average does have the correct self-consistent (SC) properties, and so we use that, which yields

$$\tau_{kk'} \approx \tau_{kk'}^{\text{SC}} \equiv \frac{\hbar}{\Delta U_{kk'}} + \frac{\hbar}{4T_{\text{vib}}}. \quad (84)$$

This is a reasonable result. The first term in Eq. (84) may be considered as a lower limit for  $\tau_{kk'}$  in an uncertainty principle sense, and it is reasonable that this provide a lower bound for Eq. (84). Furthermore, at an intersection of the potential energy surfaces, the decoherence time should be large so that the system traverses a single pass of a strong interaction region coherently, and the first term of Eq. (84) also enforces that. The second term has the effect that the decoherence term decreases to its lower limit when  $T_{\text{vib}} \rightarrow \infty$ , which is reasonable since the nuclei traverse the non-adiabatic interaction region infinitely rapidly, while in the other limit ( $T_{\text{vib}} \rightarrow 0$ ),  $\tau_{kk'}$  becomes infinite because the nuclear motion (which is ultimately responsible for decoherence) is infinitesimal. Furthermore, Eq. (84) satisfies the required limiting form of  $P_{\text{vib}}^{-2}$  for small  $P_{\text{vib}}$ , and all references to virtual hops (which were used in the derivation, but without requiring any details such as specification of the

hopping vector) are canceled out in the final expression. Based on these considerations we label  $\tau_{kk'}^{\text{SC}}$  as the fastest self-consistent time scale in the system. Clearly, the derivation of Eq. (84) is not rigorous, and hence the adoption of the geometric dependence of  $\tau_{kk'}^{\text{SC}}$ , that is contained in equation is a basic assumption of the method. The usefulness of this assumption will be tested by comparing the predictions of the new theory with various scale factors to accurate quantum-mechanical dynamics calculations.

At this point we recall a distinction emphasized in the Introduction: namely, the difference between the physical time scale of decoherence and the algorithmic time over which decay of mixing should occur so that a semiclassical ensemble of trajectories best simulates the evolution of a coherent wave packet. In deriving Eqs. (73) and (84), we focused attention on the fastest time scale in the system, which is the first term on the right side of Eq. (85). We now reiterate an important lesson of the work of Parlant and Gislason<sup>47</sup> and Thachuk *et al.*:<sup>48</sup> namely, that one obtains more accurate results if one integrates the Ehrenfest equations for the electronic amplitudes—i.e., Eqs. (13) and (14)—without interruption through each complete passage of a strong interaction region. Including the decay of mixing terms interferes with this coherent complete passage, and therefore we recognize two competing factors affecting the optimal decoherence time for the SCDM algorithm. Use of Eq. (84) gives the fastest possible self-consistent decoherence so that energy transfer between electronic degrees of freedom and nuclear degrees of freedom occurs in the region of strong coupling, which is physically reasonable. But use of this fastest possible decoherence countervenes the need for coherent complete passage of a strong coupling region. We therefore introduce a coherency factor  $C$  that makes the system more coherent, and we set

$$\tau_{kk'} = C \tau_{kk'}^{\text{SC}}. \quad (85)$$

The physical interpretation of the constant  $C$  is that it represents the factor by which first-order decay of mixing in the SCDM simulation is slower than the fastest self-consistent time scale in the system.

### II.F.3. Decoherent-state switching probability

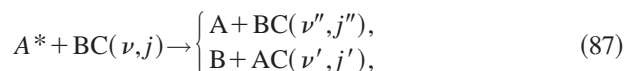
The NDM switching probability in Eq. (59) is defined in such way that when the decoherent state is  $K$ , the switching probability is also calculated from the decoherent  $K$ -state electronic density. If the decoherent state continues to be  $K$ , then  $n_K$  will approach unity and the densities in the other electronic states will tend to zero. This favors the current decoherent state because the contribution to  $\dot{n}_K$  from decoherence is always positive. Therefore the NDM switching probability is unsatisfactory. The simplest modification of the NDM switching probability that remedies this problem is to replace Eq. (59) by

$$P_{K \rightarrow K'} = \max \left( -\frac{(\dot{\rho}_{KK} - \dot{\rho}_{KK}^D)dt}{\rho_{KK}}, 0 \right) \\ = \max \left( -\frac{\dot{\rho}_{KK}^{\text{SE}}dt}{\rho_{KK}}, 0 \right). \quad (86)$$

The generalization of Eq. (86) to more than two states is straightforward, and the resulting equations are analogous to those obtained when generalizing Eq. (59), as in Ref. 22. When the switching probability is calculated from Eq. (86) or from its multistate version, the method is called self-consistent decay of mixing.

### III. TEST CASES

We test the proposed semiclassical trajectory algorithms against accurate quantum-mechanical calculations using the previously presented<sup>42,43</sup> MXH and YRH families of model potential energy matrices (PEMs). Both of these PEMs are defined in a diabatic<sup>14,36,49</sup> representation by their diagonal potential energy surfaces and their diabatic coupling surface and describe electronically nonadiabatic atom–diatom collisions of the form



where (A,B,C)=(M,H,X) and (Y, R, H) for the MXH and YRH systems, respectively; the asterisk indicates electronic excitation, and the primes on the diatomic vibrational  $\nu$  and rotational  $j$  quantum numbers indicate that these quantities need not be conserved. Quantum-mechanical calculations have been carried out<sup>42,43</sup> using these model systems for several different initial conditions and total energies, and we consider a subset of the cases here. We will label the initial conditions by the total energy  $E$  given in eV and the initial rotational state  $j$  of the diatomic molecule [i.e., by  $(E/\text{eV}, j)$ ]. For all of the cases considered here, the diatom is initially in its ground vibrational state (i.e.,  $\nu=0$ ), and the total angular momentum of the system is zero. In total, we will consider nine cases involving three surfaces of the MXH type and three cases involving two surfaces of the YRH type.

The YRH PEMs feature weakly coupled, nearly parallel potential energy surfaces in the entrance valley (i.e., as Y\* approaches RH) and may be considered Rosen–Zener–Demkov systems.<sup>50–52</sup> The masses of the Y, R, and H atoms are 10, 6, and 1.007 83 amu, respectively. Three YRH cases are included in the test set (where “case” is used to denote a specific member of the YRH or MXH family—i.e., a specific PEM parametrization—coupled with a specific set of initial conditions): the YRH(0.1) parametrization with the (1.10, 0) initial conditions and the YRH(0.2) parametrization with the (1.02, 0) and (1.10, 6) initial conditions. Details of the YRH parametrizations and initial conditions are given in Ref. 43. This subset of three YRH cases was used in place of the previously published<sup>43</sup> set of 12 YRH cases because we showed for a subset of the methods tested that one draws reasonably similar conclusions from a subset, and so it is not necessary to consider all 12 cases to test the methods, especially considering the higher expense<sup>53</sup> of studying weakly coupled systems. The three YRH cases included in the

present study were selected such that trends in error estimates obtained using the subset of three YRH cases were similar to those obtained with the full set of 12 YRH cases for several previously published semiclassical results<sup>43</sup> while maintaining some variety in the test set.

The MXH PEMs feature a narrowly avoided crossing and a localized region of strong coupling and may be considered Landau–Zener–Teller systems.<sup>54–57</sup> The masses of the M, H, and X model atoms are 6.046 95, 1.007 83, and 2.015 65 amu, respectively. The SB (strong broad), SL (strong localized), and WL (weak localized) parametrizations of the MXH system with the (1.10, 0), (1.10, 1), and (1.10, 2) initial conditions were included in the test set for a total of nine MXH cases. Details of the MXH parametrizations and initial conditions are given in Ref. 21.

The quantum-mechanical observables for the YRH and MXH parametrizations considered here exhibit an oscillatory structure as functions of scattering energy.<sup>42,43</sup> We have previously found that semiclassical results depend only slowly on energy.<sup>42,43</sup> It is therefore desirable to compare the semiclassical results obtained at a single-scattering energy to the average quantum-mechanical value obtained over a range of energies. Quantum-mechanical calculations were performed at seven energies at and around the nominal scattering energies for YRH (see the supporting information of Ref. 43 for details) and 14 energies at and around the nominal scattering energy for MXH (see the supporting information of Ref. 42 for details). The results of the quantum-mechanical calculations were averaged to obtain the quantum results used here. In most cases, the values obtained by averaging are similar to the values obtained at the nominal scattering energy.

### IV. SEMICLASSICAL TRAJECTORY CALCULATIONS

The coordinates and momenta of the nuclei and the electronic state populations were integrated using an adaptive integration algorithm that was designed for use with semiclassical trajectory calculations.<sup>39</sup> The algorithm uses a Bulirsch–Stoer integrator with polynomial extrapolation<sup>58,59</sup> modified such that the integrator is prohibited from stepping over local peaks and minima in the electronic probabilities.<sup>59</sup> For the present calculations, the integration parameters<sup>59</sup> were given the following values:  $\epsilon_{\text{BS}} = 10^{-12} E_h$  ( $1 E_h = 27.211$  eV) and  $h_{\text{min}} = 10^{-4}$  a.u. ( $1 \text{ a.u.} = 2.4189 \times 10^{-2}$  fs), which give converged results for the YRH and MXH systems. The trajectories begin the simulation with the lone atom (Y in the case of YRH and M in the case of MXH) separated from the center of mass of the diatom by  $35a_0$  ( $1a_0 = 0.529 18 \text{ \AA}$ ) for the MXH cases and by  $20a_0$  for the YRH cases, and the simulation was ended when the product fragments were separated by at least  $30a_0$  for both systems. We have verified that the results of the semiclassical simulations do not change when these distances are increased.

The results are sometimes sensitive to the method used to compute  $P_{K \rightarrow K'}$  in Eqs. (59) and (86). One obtains better convergence with respect to decreasing  $dt$  if  $\dot{\rho}_{kk}(t)dt$  is replaced by  $\rho_{kk}(t) - \rho_{kk}(t-dt)$ .

In addition to testing the new SCDM method, we will present the results of semiclassical trajectory calculations

TABLE I. Semiclassical trajectory methods tested in this paper.

Method	Ref.	Explanation
TFS–	22	The original version of Tully's fewest switches (TFS) algorithm for trajectory surface hopping. The minus denotes that the trajectory is reflected at frustrated hops.
FSTUVV	60, 61	The fewest switches with time uncertainty (FSTU) algorithm for trajectory surface hopping. The VV suffix denotes that frustrated hops are treated by the grad $V$ algorithm.
SE–H	15, 19, 62	Semiclassical Ehrenfest method with histogram analysis for final states
SE–LSS	15, 19, 62	Semiclassical Ehrenfest method with linear smooth sampling analysis for final states
NDM	21, 23	Original natural decay of mixing method
NDM/SCDT	Present	NDM with self-consistent (SC) direction (D) and time (T)—i.e., Eqs. (67) and (85) instead of Eqs. (55) and (56), respectively
NDM/SCS	Present	NDM with self-consistent (SC) switching (S)—i.e., Eq. (86) instead of Eq. (59)
SCDM	Present	Self-consistent decay of mixing as presented in Sec. II F of the present paper

employing several other methods<sup>15,19,21–23,60–62</sup> for comparison. In particular, the methods tested are listed and explained in Table I.

Note that each method in Table I can be implemented in the adiabatic representation (e.g., FSTUVV-A), the diabatic representation (e.g., FSTUVV-D), or the Calaveras County representation (e.g., FSTUVV-CC). The Calaveras County (CC) representation<sup>13</sup> involves choosing for each case (potential energy surfaces and couplings, masses, energy, initial vibrational–rotational state) between the A or D representation on the basis of which representation leads to the fewest number of hop attempts per trajectory (on average) in a TFS calculation. We previously presented arguments<sup>13,19</sup> that this is the best representation for trajectory surface hopping, and we also propose it as a reasonable way to choose a representation in decay-of-mixing calculations. For the 12 cases considered here, for 9 of them (SB, SL, and YRH) the CC representation turns out to be the adiabatic one, and only for the three WL cases does it turn out to be the diabatic representation.

We note that the numerical method used for NDM and NDM/SCS (see Table I for method acronyms) adiabatic calculations is that presented in Ref. 23, whereas the formulation used for the NDM/SCDT and SCDM adiabatic calculations is that presented in the present paper; however, the results are independent of this methodological choice. The semiclassical Ehrenfest method yields the same results in the diabatic representation or in the adiabatic representation of Ref. 23. For a two-state case, results in the diabatic representation agree with those obtained using either adiabatic representation. So, for the two-state systems considered here no representation needs to be specified.

The semiclassical trajectory calculations yield eight quantities that will be compared to the accurate quantum-mechanical results summarized in Sec. III. In particular, we calculate  $P_R$ , the probability of reaction, which is the lower outcome in Eq. (87);  $P_Q$ , the probability of quenching, which is the top outcome in Eq. (87);  $P_N$ , the total probabil-

ity of a nonadiabatic event, which is the sum of  $P_R$  and  $P_Q$ ;  $F_R$ , the reactive branching fraction, which is defined as  $P_R/P_N$ ;  $\langle \nu' \rangle$ , the mean value of  $\nu'$  in Eq. (87);  $\langle j' \rangle$ , the mean value of  $j'$  in Eq. (87);  $\langle \nu'' \rangle$ , the mean value of  $\nu''$  in Eq. (87); and  $\langle j'' \rangle$ , the mean value of  $j''$  in Eq. (87).

For the SE calculations, the final-state analysis is carried out using both the histogram (H) and linear smooth sampling (LSS) methods (without taking account of whether states are closed), as presented previously.<sup>19,62</sup> For all other calculations we employed only histogram analysis.

## V. RESULTS

First, we gathered statistics to compare the time-averaged decoherence rates calculated by the original NDM approximation with Eq. (56) to those calculated with the new self-consistent expression, Eq. (85). The decoherence time is not meaningful in the initial and final legs of the trajectories (asymptotic regions) where the coupling is essentially zero. Thus we only averaged over portions of the trajectories where  $0.02 \leq n_k \leq 0.98$ . To average the rates, we calculated the time average of  $1/\tau_{12}$  for this portion of each trajectory and then averaged these values over the ensemble of trajectories. Then the result is reexpressed in time units by taking a reciprocal:

$$\bar{\tau} \equiv \frac{1}{\langle 1/\tau_{12} \rangle}. \quad (88)$$

The resulting values, called the time-averaged decoherence times, are shown for three cases in Table II.

Table II shows that the original formula (used in NDM) gives time-averaged decoherence times of 2.5–8 fs in the adiabatic representation and 2.9–10 fs in the diabatic representation. The self-consistent formula is less dependent on representation, and using  $C=1$ , which corresponds to the shortest self-consistent decoherence time, gives very fast decay of mixing, with  $\bar{\tau}=1.5$ –3.2 fs. These values then increase roughly proportional to  $C$ , becoming 13–27 fs for  $C=9$ .

TABLE II. Average decoherence times  $\tau$  (in fs).

Method	C	Rep.	MXH SB	MXH WL	YRH 0.2
			$j=2$	$j=1$	1.02 eV, $j=0$
NDM	...	A	2.5	3.7	8.0
		D	3.3	2.9	10
NDM/SCDT	1	A	1.5	2.4	2.3
	1	D	1.8	1.8	3.2
	3	A	4.5	5.5	7.7
	3	D	5.3	4.7	9.1
	6	A	8.9	9.7	16
	6	D	10.	9.0	18
	9	A	13	14	27
	9	D	15	13	27
NDM/SCS	...	A	2.5	3.7	7.6
		D	3.4	2.9	11
SCDM	1	A	1.5	2.7	2.3
	1	D	1.9	1.8	3.2
	3	A	4.5	5.7	7.3
	3	D	5.4	4.7	9.2
	6	A	8.9	9.7	16
	6	D	10.	8.9	18
	9	A	13	14	27
	9	D	15	13	27

Limiting the averages to only quenching trajectories or only the subset of reactive trajectories or the subset of quenching trajectories did not produce any systematic differences for MXH with time-averaged decoherence times for each of the subsets sometimes being within  $\sim 10\%$  of those for the full set and being sometimes smaller and sometimes larger than for the full set. For YRH, though,  $\bar{\tau}$  for reactive trajectories is as much as 48% less than the time average over all trajectories and  $\bar{\tau}$  for quenching trajectories is up to 36% less than the time average over all trajectories.

In order to test the accuracy of the methods we computed the unsigned relative error in each of the eight quantities specified in Sec. IV:

$$\varepsilon_{i\alpha} = \frac{|Q_{i\alpha}^{\text{traj}} - Q_{i\alpha}^{\text{quantal}}|}{Q_{i\alpha}^{\text{quantal}}}, \quad (89)$$

where  $Q_{i\alpha}$  is quantity  $i$  for test case  $\alpha$ . The first four quantities are called branching probabilities, and the mean unsigned error in these is

$$\bar{\varepsilon}_a(\text{prob}) = \frac{1}{4} \sum_{i=1}^4 \sum \varepsilon_{i\alpha}, \quad (90)$$

whereas the next four quantities are called final-state moments and the mean unsigned error in these is

$$\bar{\varepsilon}_\alpha(\text{mom}) = \frac{1}{4} \sum_{i=5}^8 \varepsilon_{i\alpha}. \quad (91)$$

These were then averaged over the nine MXH cases and converted to percentage errors

$$\text{PE}(X; \text{MXH}) = \frac{100}{9} \sum_{\alpha=1}^9 \bar{\varepsilon}_\alpha(X) \quad (92)$$

and similarly for the three YRH cases

TABLE III. Mean unsigned relative errors (%) in branching probabilities and final-state moments.

Method	C	Rep.	MXH		YRH		Average
			prob	mom	prob	mom	
NDM/SCDT	1	A	63	19	63	26	43
	1	D	45	20	164	27	64
	3	A	42	24	41	27	34
	3	D	32	21	191	29	68
	6	A	34	23	30	28	29
	6	D	33	21	178	31	66
	9	A	39	22	22	29	28
	9	D	39	19	154	34	61
SCDM	1	A	51	27	29	25	33
	1	D	43	19	249	29	85
	3	A	32	25	34	25	29
	3	D	31	21	135	31	54
	6	A	28	24	29	27	27
	6	D	33	21	90	33	44
	9	A	34	22	24	28	27
	9	D	37	19	66	37	40

$$\text{PE}(X; \text{YRH}) = \frac{100}{3} \sum_{\alpha=10}^{12} \bar{\varepsilon}_\alpha(X), \quad (93)$$

where  $X=1$  = “prob” and  $X=2$  = “mom.” Finally, we averaged the two types of errors and two types of systems to obtain “average” mean unsigned errors

$$\text{PE}(\text{average}) = \frac{1}{2} \sum_{X=1}^2 \frac{\text{PE}(X, \text{MXH}) + \text{PE}(X, \text{YRH})}{2}. \quad (94)$$

We can also average in the other order, obtaining

$$\langle \varepsilon_i \rangle = \frac{\sum_{\alpha=\beta}^{\gamma} \varepsilon_{i\alpha}}{\gamma - \beta + 1}. \quad (95)$$

For a complete set of results, including  $Q_{i\alpha}^{\text{quantal}}$  and  $Q_{i\alpha}^{\text{traj}}$  for all of the semiclassical methods and test cases considered in this paper, as well as  $\langle \varepsilon_i \rangle$  for MXH ( $\beta=1$ ,  $\gamma=9$ ) and YRH ( $\beta=10$ ,  $\gamma=12$ ) and various other averages of these quantities, see the supporting information.<sup>63</sup> Here we focus on the more highly averaged percentage errors of Eqs. (92)–(94) because these are sufficient to test the performances of the methods. These percentage errors are given in Tables III and IV.

Table III is a test of how the accuracy depends on  $C$ . We see that the average percentage errors decrease considerably when  $C$  is increased from 1 to 3, and they further decrease as  $C$  is increased to 6, but the results for  $C=6$  and  $C=9$  are similar. For YRH, the error in the moments increases with increasing  $C$ , but the opposite trend is found for MXH. For YRH the errors in the probabilities decrease systematically as  $C$  is increased from 1 to 9, whereas for MXH they show a minimum at  $C=6$ . If one were to continue to increase  $C$  to  $\infty$ , the probabilities should tend to the EH–LSS values, and the moments should become inaccurate (since energy would be transferred into or out of electronic degrees of freedom only very slowly in the distant post-collision asymptotic region where the coupling is essentially zero).



TABLE IV. Mean unsigned relative errors (%) in branching probabilities and final-state moments.

Method	<i>C</i>	Rep.	MXH		YRH		Average
			prob	mom	prob	mom	
TFS–	...	A	56	17	40	46	40
	...	D	46	18	458	55	144
	...	CC	53	18	40	46	39
FSTUVV	...	A	53	18	27	46	36
	...	D	43	18	202	62	81
	...	CC	48	17	27	46	35
SE–H	...	all	50	34	98	47	72
SE–LSS	...	all	51	30	68	83	75
NDM	...	A	53	27	36	23	35
	...	D	36	24	211	23	73
	...	CC	48	27	36	23	33
NDM/SCDT	9	A	39	22	22	29	28
	9	D	39	19	154	34	61
	9	CC	41	20	22	29	28
NDM/SCS	...	A	48	26	28	21	31
	...	D	36	22	117	24	50
	...	CC	45	26	28	21	30
SCDM	9	A	34	22	24	28	27
	9	D	37	19	66	37	40
	9	CC	38	21	24	28	28

All things considered, the optimum value of *C* is probably in the range 6–9. We will use *C*=9 since Table III shows this is slightly better than *C*=6 on average.

An interesting aspect of the results in Table III is that the dependence on choice of representation gets smaller as *C* increases. This is reasonable since in the Ehrenfest limit, *C* = ∞ and the results are fully independent of representation.

Table IV compares the performance of the SCDM results with *C*=9 to previously available methods and to two methods intermediate between NDM and SCDM. We will next consider these result in the order that they appear in the table.

The TFS– method defines a useful base line for testing the accuracy of proposed improved methods. TFS– shows reasonable accuracy in both representations for MXH, but very poor accuracy in the diabatic representation for YRH. This is probably a good place to explain why representation independence is important. First, “for general multidimensional problems, the evaluation of the optimal representation poses serious numerical problems.”<sup>64</sup> Second, even if one restricts oneself to choosing between the adiabatic and diabatic representations, it is not always possible to predict (when the accurate quantal results are unavailable) which representation is preferred. Third, and even more important, is that for complex systems there could be regions of configuration space in which the adiabatic representation is preferred, but for the same system with the same initial conditions, there could be other regions of configuration space where the diabatic representation is more natural. The results for general complex systems should be much more reliable if one has a method that yields accurate results in both representations.

The next method in Table IV, FSTUVV, is, as expected<sup>60,61</sup> more accurate than TFS–. Encouragingly, its accuracy is also less dependent on representation, but the YRH probabilities still have large errors when this system is treated diabatically.

The trajectories of the SE method, unlike those of the surface hopping and decay-of-mixing methods, do not end in a pure electronic state. This causes the amount of energy available for translation, rotation, and vibration to be unphysical, and this is reflected in the large errors in the rotational and vibrational moments. One can somewhat ameliorate these errors by histogramming, but this can significantly raise the errors in the probabilities.

The next method in the table is NDM. On average NDM is already better than TFS–, FSTUVV, and SE. Not only are the results better than all three of these previous methods, but the accuracy is also less dependent on representation. This good performance is one reason why we decided to further explore the DM approach, leading to the present paper.

Moving from NDM to NDM/SCDT or NDM/SCS corresponds to adding the first two or the third of the three improvements of the present paper. It is very encouraging that when either subset of these improvements—namely, the direction of energy release and the geometry dependence of the decoherence time (in NDM/SCDT) and making the switching algorithm consistent with time-dependent Hartree theory (in NDM/SCS)—is introduced individually, the accuracy improves very significantly.

Finally, Table IV shows even more improvement when all three self-consistent improvements are introduced in the full SCDM method. In fact, looking back at Table III for a moment, even the less optimum value of *C*=6 provides better accuracy than NDM/SCS or NDM/SCDT (with any value of *C*), and even the far-from-optimum value of *C*=3 is better than the original NDM, which was our best method prior to the present paper.

We do not have a good theoretical reason for choosing a particular value of *C*. The results presented here, along with extensive (unpublished) tests on one-dimensional model systems, show that the results usually improve as *C* is increased from 1 to 6, but show little change from 6 to 9. Thus *C* = 6–9 seems to be a stable region, and we recommend choosing *C* in this region. That is we want *C* to be the smallest value that gives accurate state populations so that energy release occurs mainly in the strong-coupling region. If we make *C* too large, the energy transfer may be delayed to a less strongly coupled region, which is unphysical. This gives insight into a limitation of the semiclassical Ehrenfest method, which is analogous to *C*=∞. If, on the contrary, we make *C* too small, the electronic amplitudes are typically not treated as coherent over even a single transversal of a strong-coupling region, and the state probabilities evolve less self-consistently and (according to our tests) less accurately. This gives insight into a limitation of the fewest-switches trajectory surface hopping method, which is analogous to *C*=0 at the places here hops occur. The surface hopping method of Parlant and Gislason<sup>6,7,47</sup> attempts to remove this limitation, but at the cost of requiring one to rerun certain portions of the trajectory.

## VI. CONCLUDING REMARKS

In this article, we modified the natural decay of mixing algorithm in three ways to make the method more consistent with the time-dependent Hartree method. At the same time

we retained the key concept of first-order decay of mixing, which is required to obtain physical final states. The resulting new method, called self-consistent decay of mixing (SCDM), may be regarded from two different points of view. On the one hand, it corresponds to including decay of mixing in the time-dependent Hartree method so that each trajectory has a physical final electronic state and corresponds to a reasonably unmixed state at the start of each traversal of successive transversals of the strong-coupling regions in a single trajectory. On the other hand, the algorithm corresponds to smearing-out a trajectory surface hop so that it occurs no faster than the fastest self-consistent time scale in the system, rather than treating it as instantaneous. This SCDM method is tested against accurate quantal dynamics for 12 cases on 5 different sets of potential energy surfaces. It is very encouraging that the theoretical improvements, whether introduced separately or together, result in improved agreement, on average, with the accurate quantum-mechanical results (see the last column of the last three rows of Table IV). In the process we have further improved the reliability of semiclassical trajectory methods for treating non-Born–Oppenheimer dynamics, and we believe that our method should be very useful for simulations of photochemical reactions.

Although our explicit attention has been restricted to treatments where all electronic degrees of freedom are treated quantum mechanically and nuclear degrees of freedom are treated classically (or quasiclassically), semiclassical Ehrenfest-like methods have also been used to treat a subset of nuclear motion quantum mechanically,<sup>8,18,20,65,66</sup> and the SCDM method for combining quantum mechanics and classical mechanics may also be useful for that case.

## ACKNOWLEDGMENTS

The authors are grateful to Amos Anderson for assistance with some of the calculations. This work was supported in part by the National Science Foundation under Grant No. CHE00-92019.

## APPENDIX: DERIVATION OF EHRENFEST HAMILTONIAN IN THE ADIABATIC CASE

In the adiabatic representation,  $U_{kk'}=0$  if  $k \neq k'$  and  $U_{kk}=V_k$ . Therefore, from Eq. (8),

$$\dot{H}^{\text{SE}} = \dot{\mathbf{R}} \cdot \dot{\mathbf{P}} + \sum_k n_k \dot{V}_k + \sum_k \dot{n}_k V_k, \quad (\text{A1})$$

where we used the fact that  $\mathbf{P} = \mu \dot{\mathbf{R}}$ , and an overdot denotes a time derivative. Semiclassically, we have

$$\dot{V}_k = \dot{\mathbf{R}} \cdot \nabla_{\mathbf{R}} V_k, \quad (\text{A2})$$

and using Eqs. (10), (43), and (44) yields

$$\dot{n}_k = - \left( x_k \sum_k x_{k'} \dot{\mathbf{R}} \cdot \mathbf{d}_{kk'} + p_k \sum_{k'} p_{k'} \dot{\mathbf{R}} \cdot \mathbf{d}_{kk'} \right). \quad (\text{A3})$$

Substituting Eqs. (A2) and (A3) into Eq. (A1) yields

$$\begin{aligned} \dot{H}^{\text{SE}} = & \dot{\mathbf{R}} \cdot \left( \dot{\mathbf{P}} + \sum_k n_k \nabla_{\mathbf{R}} V_k \right. \\ & \left. - \sum_k \sum_{k'} (x_k x_{k'} + p_k p_{k'}) V_k \mathbf{d}_{kk'} \right). \end{aligned} \quad (\text{A4})$$

Since energy must be conserved, this must equal zero. Since  $\dot{\mathbf{R}}$  is not zero, in general,

$$\dot{\mathbf{P}} = - \sum_k n_k \nabla_{\mathbf{R}} V_k + \sum_k \sum_{k'} (x_k x_{k'} + p_k p_{k'}) V_k \mathbf{d}_{kk'}. \quad (\text{A5})$$

Using Eq. (7) and the skew symmetric character of  $\mathbf{d}_{kk'}$ , one can show that Eq. (A5) agrees with Eq. (46).

A key element in the derivation presented here and in Ref. 1 is the use of the semiclassical approximation Eq. (A2). Reference 15 does not involve this semiclassical approximation, and hence the adiabatic formulation of Ref. 23, because it is based on Ref. 15, does not require it either.

- <sup>1</sup>J. C. Tully, in *Dynamics of Molecular Collisions*, edited by W. H. Miller (Plenum, New York, 1976), pt. B, p. 217.
- <sup>2</sup>D. G. Truhlar and J. T. Muckerman, in *Atom–Molecule Collision Theory: A Guide for the Experimentalist*, edited by R. B. Bernstein (Plenum, New York, 1979), p. 505.
- <sup>3</sup>L. M. Raff and D. L. Thompson, in *Theory of Chemical Reaction Dynamics*, edited by M. Baer (CRC, Boca Raton, FL, 1985), Vol. 3, p. 1.
- <sup>4</sup>E. E. Nikitin, *Theory of Elementary Atomic and Molecular Processes in Gases* (Clarendon, Oxford, 1974), Chap. 3.
- <sup>5</sup>M. S. Child, in *Atom–Molecule Collision Theory: A Guide for the Experimentalist*, edited by R. B. Bernstein (Plenum, New York, 1979), p. 427.
- <sup>6</sup>E. A. Gislason, G. Parlant, and M. Sizun, *Adv. Chem. Phys.* **82**, 321 (1992).
- <sup>7</sup>S. Chapman, *Adv. Chem. Phys.* **82**, 423 (1992).
- <sup>8</sup>G. D. Billing, *Int. Rev. Phys. Chem.* **13**, 309 (1994).
- <sup>9</sup>H. Nakamura, in *Dynamics of Molecules and Chemical Reactions*, edited by R. E. Wyatt and J. Z. H. Zhang (Dekker, New York, 1996), p. 473.
- <sup>10</sup>J. C. Tully, in *Modern Methods for Multidimensional Dynamics Calculations*, edited by D. L. Thompson (World Scientific, Singapore, 1998), p. 34.
- <sup>11</sup>D. A. Micha, *Adv. Quantum Chem.* **35**, 317 (1999).
- <sup>12</sup>J. Mavri, *Mol. Simul.* **23**, 389 (2000).
- <sup>13</sup>M. D. Hack and D. G. Truhlar, *J. Phys. Chem. A* **104**, 7917 (2000).
- <sup>14</sup>A. W. Jasper, B. K. Kendrick, C. A. Mead, and D. G. Truhlar, in *Modern Trends in Chemical Reaction Dynamics*, edited by X. Yang and K. Liu (World Scientific, Singapore, in press).
- <sup>15</sup>H.-D. Meyer and W. H. Miller, *J. Chem. Phys.* **70**, 3214 (1979).
- <sup>16</sup>D. A. Micha, *J. Chem. Phys.* **78**, 7138 (1983).
- <sup>17</sup>M. Amarouche, F. X. Gadea, and J. Durup, *Chem. Phys.* **130**, 145 (1989).
- <sup>18</sup>A. Garcia-Vela, R. B. Gerber, and D. G. Imre, *J. Chem. Phys.* **97**, 7242 (1992).
- <sup>19</sup>M. S. Topaler, T. C. Allison, D. W. Schwenke, and D. G. Truhlar, *J. Chem. Phys.* **109**, 3321 (1998); **113**, 3928(E) (2000).
- <sup>20</sup>A. Alimi, R. B. Gerber, A. D. Hammerlich, R. Kosloff, and M. A. Ratner, *J. Chem. Phys.* **93**, 6484 (1990).
- <sup>21</sup>M. D. Hack and D. G. Truhlar, *J. Chem. Phys.* **114**, 9305 (2001).
- <sup>22</sup>J. C. Tully, *J. Chem. Phys.* **93**, 1061 (1990).
- <sup>23</sup>A. W. Jasper, M. D. Hack, A. Chakraborty, D. G. Truhlar, and P. Piecuch, *J. Chem. Phys.* **115**, 7945 (2001); **119**, 9321(E) (2003).
- <sup>24</sup>A. W. Jasper, A. G. Anderson, and D. G. Truhlar (unpublished).
- <sup>25</sup>A. Bohm, *Quantum Mechanics: Foundations and Applications*, 3rd ed. (Springer-Verlag, New York, 1993), pp. 57–73.
- <sup>26</sup>B. J. Schwarz, E. R. Bittner, O. V. Prezhdo, and P. J. Rossky, *J. Chem. Phys.* **104**, 5942 (1996).
- <sup>27</sup>O. V. Prezhdo and P. J. Rossky, *J. Chem. Phys.* **107**, 5863 (1997).
- <sup>28</sup>K. F. Wong and P. J. Rossky, *J. Chem. Phys.* **116**, 8429 (2002).
- <sup>29</sup>(a) O. V. Prezhdo and P. J. Rossky, *J. Chem. Phys.* **107**, 825 (1997); (b) K. F. Wong and P. J. Rossky, *J. Phys. Chem. A* **105**, 2546 (2001).

- <sup>30</sup>C. C. Martens and J. Y. Fang, J. Chem. Phys. **106**, 4918 (1997).
- <sup>31</sup>J. C. Burant and J. C. Tully, J. Chem. Phys. **112**, 6097 (2000).
- <sup>32</sup>M. Santer, U. Manthe, and G. Stock, J. Chem. Phys. **114**, 2001 (2001).
- <sup>33</sup>H.-D. Meyer and W. H. Miller, J. Chem. Phys. **72**, 2272 (1980).
- <sup>34</sup>M. Karplus, R. N. Porter, and R. D. Sharma, J. Chem. Phys. **43**, 3529 (1965).
- <sup>35</sup>G. C. Schatz, M. T. Horst, and T. Takayanagi, in *Modern Methods for Multidimensional Dynamics Calculations*, edited by D. L. Thompson (World Scientific, Singapore, 1998), p. 1.
- <sup>36</sup>C. A. Mead and D. G. Truhlar, J. Chem. Phys. **77**, 6090 (1982).
- <sup>37</sup>B. K. Kendrick, C. A. Mead, and D. G. Truhlar, Chem. Phys. Lett. **330**, 629 (2000).
- <sup>38</sup>B. K. Kendrick, C. A. Mead, and D. G. Truhlar, Chem. Phys. **277**, 31 (2002).
- <sup>39</sup>M. D. Hack, A. W. Jasper, Y. L. Volobuev, D. W. Schwenke, and D. G. Truhlar, J. Phys. Chem. A **103**, 6309 (1999).
- <sup>40</sup>R. W. Numrich and D. G. Truhlar, J. Phys. Chem. **79**, 2745 (1975).
- <sup>41</sup>S. L. Mielke, G. J. Tawa, D. G. Truhlar, and D. W. Schwenke, Chem. Phys. Lett. **234**, 57 (1995).
- <sup>42</sup>Y. L. Volobuev, M. D. Hack, M. S. Topaler, and D. G. Truhlar, J. Chem. Phys. **112**, 9716 (2000).
- <sup>43</sup>A. W. Jasper, M. D. Hack, and D. G. Truhlar, J. Chem. Phys. **115**, 1804 (2001).
- <sup>44</sup>H. Nakamura and D. G. Truhlar, J. Chem. Phys. **115**, 8460 (2001).
- <sup>45</sup>M. F. Herman, J. Chem. Phys. **81**, 754 (1984).
- <sup>46</sup>D. F. Coker and L. Xiao, J. Chem. Phys. **102**, 496 (1995).
- <sup>47</sup>G. Parlant and E. A. Gislason, J. Chem. Phys. **91**, 4416 (1989).
- <sup>48</sup>M. Thachuk, M. Y. Ivanov, and D. M. Wardlaw, J. Chem. Phys. **109**, 5747 (1998).
- <sup>49</sup>A. D. McLachlan, Mol. Phys. **4**, 417 (1961).
- <sup>50</sup>N. Rosen and C. Zener, Phys. Rev. **18**, 502 (1932).
- <sup>51</sup>Yu. N. Demkov, Zh. Eksp. Teor. Fiz. **45**, 195 (1963) [Sov. Phys. JETP **18**, 138 (1966)].
- <sup>52</sup>Yu. N. Demkov, Dokl. Akad. Nauk SSSR **166**, 1076 (1966) [Sov. Phys. Dokl. **11**, 138 (1966)].
- <sup>53</sup>S. Nangia, A. W. Jasper, T. F. Miller III, and D. G. Truhlar, J. Chem. Phys. **120**, 3586 (2004).
- <sup>54</sup>L. D. Landau, Phys. Z. Sowjetunion **2**, 46 (1932).
- <sup>55</sup>C. Zener, Proc. R. Soc. London, Ser. A **137**, 696 (1932).
- <sup>56</sup>E. C. G. Stückelberg, Helv. Phys. Acta **5**, 369 (1932).
- <sup>57</sup>E. Teller, J. Phys. Chem. **41**, 109 (1937).
- <sup>58</sup>W. H. Press, S. A. Teukolsky, W. T. Vetterling, and B. P. Flannery, *Numerical Recipes in FORTRAN*, 2nd ed. (Cambridge University Press, Cambridge, UK, 1994), pp. 716–725.
- <sup>59</sup>M. S. Topaler, M. D. Hack, T. C. Allison, Y.-P. Liu, S. L. Mielke, D. W. Schwenke, and D. G. Truhlar, J. Chem. Phys. **106**, 8699 (1997).
- <sup>60</sup>A. W. Jasper, S. N. Stechmann, and D. G. Truhlar, J. Chem. Phys. **116**, 5424 (2002); **117**, 10427(E) (2002).
- <sup>61</sup>A. W. Jasper and D. G. Truhlar, Chem. Phys. Lett. **369**, 60 (2003).
- <sup>62</sup>M. D. Hack, A. W. Jasper, Y. L. Volobuev, D. W. Schwenke, and D. G. Truhlar, J. Phys. Chem. A **104**, 217 (2000).
- <sup>63</sup>See EPAPS Document No. E-JCPSA6-120-019411 for tables containing detailed semiclassical trajectory and quantum mechanical results for all of the methods and cases summarized in the present work, as well as tables featuring various mean unsigned errors. A direct link to this document may be found in the online article's HTML reference section. The document may also be reached via the EPAPS homepage (<http://www.aip.org/pubservs/epaps.html>) or from <ftp.aip.org> in the directory /epaps/. See the EPAPS homepage for more information.
- <sup>64</sup>M. F. Herman, J. Chem. Phys. **110**, 4141 (1999).
- <sup>65</sup>H. Wang, M. Thoss, and W. H. Miller, J. Chem. Phys. **115**, 2979 (2001).
- <sup>66</sup>M. I. Hernandez, A. Garcia-Vela, J. Campos-Martinez, O. Roncero, P. Villareal, and G. Delgado-Barrio, Comput. Phys. Commun. **145**, 97 (2002).